CNAD: A Potent and Specific Inhibitor of Alcohol Dehydrogenase

Barry M. Goldstein,*,† Hong Li,† Jeffrey P. Jones,‡ J. Ellis Bell,§ Joanna Zeidler,⊥ Krzysztof W. Pankiewicz,⊥ and Kyoichi A. Watanabe⊥

Departments of Biophysics and Pharmacology, University of Rochester Medical Center, Rochester, New York 14642, Departments of Chemistry and Biology, Gustavus Adolphus College, St. Peters, Minnesota 56082, and Sloan-Kettering Division of Graduate School of Medical Sciences, Memorial Sloan-Kettering Cancer Center, Sloan-Kettering Institute for Cancer Research, Cornell University, New York, New York 10021

Received August 5, 1993®

CNAD (5-β-D-ribofuranosylnicotinamide adenine dinucleotide) is an isosteric and isomeric analogue of NAD, in which the nicotinamide ring is linked to the sugar via a C-glycosyl (C5–C1′) bond. CNAD acts as a general dehydrogenase inhibitor but shows unusual specificity and affinity for liver alcohol dehydrogenase (ADH, EC 1.1.1.1). The pattern of inhibition is competitive, with $K_i \simeq 4$ nM, with NAD as the variable substrate. These values are 3–5 orders of magnitude smaller than those obtained for CNAD in other dehydrogenases and are comparable to values observed for the tightest binding ADH inhibitors known. The specificity and affinity of CNAD for ADH are likely due to coordination of the zinc cation at the ADH catalytic site by the CNAD pyridine nitrogen. This is supported by kinetic and computational studies of ADH–CNAD complexes. These results are compared with those for a related analogue, CPAD. In this analogue, displacement of the pyridine nitrogen to the opposite side of the ring removes the specificity for ADH.

Introduction

The specificity of binding by a small ligand to an enzyme is influenced by a host of intra- and intermolecular interactions. In general, these will involve the enzyme, the ligand, and the solvent and may produce a variety of conformational changes in each system.[1] Both the number and the variety of potential interactions involved in this process may be large. It is thus of interest when observed differences in binding affinity among several ligands can be attributed to a specific structural change and these in turn can be associated with differences in a single interaction. Examination of dehydrogenase binding by the cofactor analogues discussed below offers a potential example.

Nicotinamide adenine dinucleotide (NAD[2]) is a ubiquitous cofactor. In its oxidized and reduced forms, NAD serves as a hydride-ion acceptor and donor, respectively, and is thus instrumental in catalyzing hydride transfer in dehydrogenase enzymes.[3] In an attempt to target dehydrogenases involved in cell proliferation and differentiation, a number of analogues of NAD have been synthesized as potential inhibitors with chemotherapeutic activity.[4-6] An example of one such agent is CNAD (5-β-D-ribofuranosylnicotinamide adenine dinucleotide, Figure 1a). This is an isosteric and isomeric analogue to NAD, in which the nicotinamide ring is linked to the sugar via a C-glycosyl (C5–C1′) bond.[6] The pyridine base in CNAD is neutral and aromatic, thus sharing features with both the pyridinium ring in the oxidized cofactor (Figure 1b) and the dihydronicotinamide ring in the reduced cofactor NADH (Figure 1c). The structural similarity between the analogue and the natural cofactors is obvious. However, the uncharged pyridine ring in CNAD is resistant to hydride reduction, allowing the analogue to function as a dehydrogenase inhibitor.

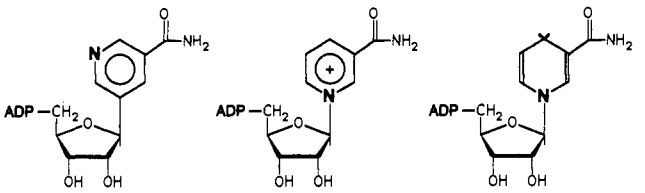

Figure 1. Cofactor analogue CNAD (a) shares features with both oxidized (b) and reduced (c) NAD.

In order to examine the relative ability of CNAD to act as a general dehydrogenase inhibitor, inhibition assays were undertaken using several common enzymes. Results indicate that CNAD does act as a dehydrogenase inhibitor but displays a marked specificity for one enzyme: horse liver alcohol dehydrogenase (ADH, EC 1.1.1.1). On the basis of these data, a model of the enzyme–inhibitor complex is proposed in which CNAD mimics cofactor binding in ADH. The high affinity and specificity of CNAD for ADH are attributed to the interaction between the pyridine nitrogen and the catalytic site Zn cation. Computational methods are used to quantitatively evaluate this model, which is compared to similar modes of binding of other potent ADH inhibitors.

Results and Discussion

Kinetic Studies. The ability of CNAD to inhibit mammalian alcohol, glutamate (GDH), lactate (LDH), and malate (MDH) dehydrogenases was examined. Kinetic constants (K_i's) determined using NAD as the variable substrate are summarized in Table 1 and compared with the measured K_m's for NAD.[7] K_i's for NADH using NAD as the variable substrate are also shown for GDH and ADH.

Examination of Lineweaver–Burk plots for GDH, LDH, and MDH (not shown) indicate that inhibition of these three dehydrogenases by CNAD is strictly competitive with respect to NAD. Data in Table 1 show that binding of the inhibitor to these enzymes is comparable to or weaker than that of the natural cofactor.

* Author to whom correspondence should be addressed.
† Department of Biophysics, University of Rochester Medical Center.
‡ Department of Pharmacology, University of Rochester Medical Center.
§ Gustavus Adolphus College.
⊥ Cornell University.
® Abstract published in *Advance ACS Abstracts*, December 15, 1993.

0022-2623/94/1837-0392$04.50/0

Table 1. Inhibition Constants (K_i; μM) for CNAD and Its Analogues using Various Dehydrogenases[a]

			ADH	GDH	LDH	MDH
CNAD	(NAD varied)	$K_{i(app)}$	$6(1) \times 10^{-3}$	15 (2)	188 (12)	410 (12)
		K_i	4×10^{-3}			
		K_d	$2(1) \times 10^{-3}$			
	(ETOH varied)	$K_{i(app)}$	$2.0(5) \times 10^{-3}$			
CPAD			21 (1)	50 (5)		
NADH			0.4 (3)	3.4 (4)		
NAD		K_m	25 (4)	30 (5)	141 (40)	32 (1)

[a] Numbers in parentheses are standard deviations in the last significant figure. Inhibition is with respect to NAD, unless otherwise noted.

Figure 2a shows a Lineweaver–Burk plot demonstrating inhibition of alcohol dehydrogenase by CNAD with respect to NAD. Although the simple linear fit to these data initially suggested a small intercept effect,[6] least-squares fits to the nonlinear forms of both competitive and noncompetitive rate equations are more consistent with a competitive pattern of inhibition. The inhibition constant obtained from the fit to the competitive rate equation is given in Table 1 as $K_{i(app)}$ (6 nM). This "apparent" value was obtained using the assumptions of the standard steady-state interpretation of enzyme inhibition (see the Experimental Section). However, the high affinity of CNAD for ADH requires further examination of these assumptions.

First, the nanomolar values reported here raise the possibility that equilibrium of the various enzyme–inhibitor species discussed above may not be attained, as required by a steady-state treatment. This would result from effectively irreversible binding of CNAD to ADH.[8] In this case, premixing experiments, in which the enzyme is added to CNAD prior to the addition of NAD, would initially produce very large inhibition. Over time, this inhibition would decrease, as an equilibrium between bound CNAD and NAD was reached. This equilibrium would result in an apparent increase in the rate of the measured reaction as time progressed after mixing. Despite this possibility, no such effect was observed with various premixing experiments nor was any difference in the measured rates dependent on premixing order. This indicates that either equilibrium of binding was achieved or no effective dissociation of bound CNAD occurred over the 10-min period used in the premixing experiments. Agreement between the directly measured dissociation constant and the kinetically determined inhibition constant (below) suggests that true equilibrium was achieved.

With a high-affinity inhibitor such as CNAD, it is also important to examine a second assumption of the standard steady-state treatment. This states that the total concentration of inhibitor $[I]_{total}$ is approximately equal to the concentration of free inhibitor $[I]_{free}$. This approximation requires that $[I]_{total}$ be in substantial excess of the total enzyme concentration [E]. Under this assumption, the amount of enzyme-bound inhibitor will be small compared to $[I]_{total}$ at steady state.[9,10]

The condition that $[I]_{total} \gg [E]$ cannot be satisfied in experiments examining CNAD inhibition of ADH. In these experiments, concentrations of $[I]_{total}$ comparable to [E] must be used in order to get any measurable alcohol dehydrogenase activity in the presence of CNAD. For any of the combinations of [ADH] and $[CNAD]_{total}$ used in the experiments, enzyme-bound inhibitor is potentially a significant fraction of the total inhibitor concentration $[I]_{total}$. Thus, the apparent inhibition constant $K_{i(app)}$, obtained from the steady-state treatment, becomes an upper bound of the true value.

In order to obtain an estimate of the true K_i, rate measurements were obtained at varied enzyme concentrations and the data fit to the nonlinear kinetic equation of Sculley and Morrison,[38] in which $[I]_{total} \simeq [E]$ (see the Experimental Section). The resulting estimate of the CNAD inhibition constant is listed in Table 1 as K_i (4 nM). Lastly, a direct experimental estimate of the inhibitor dissociation constant was obtained via fluorescence quenching of alcohol dehydrogenase by CNAD (see the Experimental Section). This value (2 nM), labeled K_d in Table 1, is in good agreement with the value of K_i.

It is apparent from the values in Table 1 that CNAD binds to ADH significantly more tightly than to the other dehydrogenases examined. The inhibition and dissociation constants for CNAD binding to ADH are 3–5 orders of magnitude smaller than those for CNAD binding to GDH, LDH, and MDH. Further, CNAD binds ADH with much greater affinity than does either the reduced or oxidized cofactor. Kinetic constants for CNAD binding to ADH are 2–4 orders of magnitude smaller than those for NAD and NADH. Thus, CNAD shows both high affinity and high specificity for ADH.

The influence of CNAD inhibition on ethanol binding was also studied. Figure 2b shows a Lineweaver–Burk plot for inhibition of ADH by CNAD with ethanol as the varied substrate. Again, least-squares fits of these data to the nonlinear forms of the standard steady-state rate equations are consistent with a competitive pattern of inhibition. This is likely a result of CNAD inhibition of ADH via its minor pathway (Figure 3).

The preferred mechanism for ADH is an ordered sequential mechanism in which cofactor binds first followed by ethanol substrate (Figure 3, path 1).[11] Competition for the cofactor site in this pathway by CNAD results in a binary enzyme–CNAD complex (Figure 3, path 2), producing the slope effect observed in Figure 2a. Formation of a dead-end ADH–CNAD–ethanol complex (Figure 3, path 3) would produce a noncompetitive pattern of inhibition with ethanol as the varied substrate. However, fit of the data in Figure 2b to a noncompetitive rate equation indicates that any intercept effect is relatively small, i.e., that $K_{ii} > K_{is}$. Thus, the binding of ethanol to form a ternary ADH–CNAD–ethanol complex, if it occurs, is likely to be weak.

The competitive pattern of inhibition with respect to ethanol could only be observed in the major pathway by formation of an ADH–NAD–CNAD complex. Structural considerations (below) suggest that this is highly unlikely. However, both alternate-substrate experiments[12] and isotope-exchange studies[13] with ADH clearly demonstrate the existence of a minor pathway in which ethanol binds first followed by cofactor (Figure 3, path 4). CNAD binds ADH with sufficient affinity to compete directly with ethanol in this pathway and produce the pattern of inhibition shown in Figure 2b.

Note that the data in Figure 2 demonstrate that the cofactor analogue CNAD interferes with both cofactor and substrate binding to ADH.

The ADH–CNAD Model. Kinetic data (above) indicate that the cofactor analogue CNAD acts as a general dehydrogenase inhibitor, with very high affinity and specificity for alcohol dehydrogenase. Comparison of the

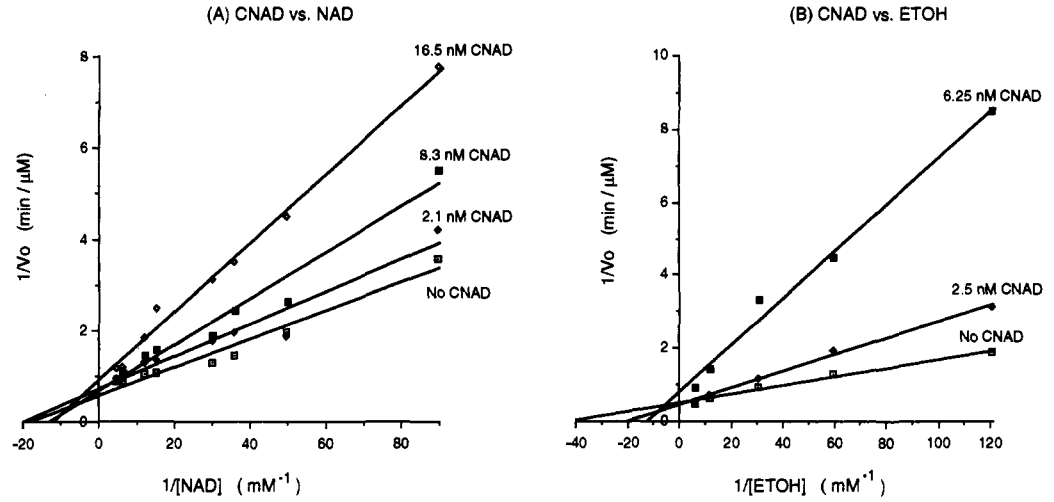

Figure 2. (A) Inhibition of alcohol dehydrogenase by CNAD with cofactor varied. NAD concentrations were varied at a fixed ethanol concentration of 1.2 mM. Assays were performed as described in the Experimental Section at pH 8.0 using 2.8 nM ADH in the absence of CNAD (□) or in the presence of 2.1 nM CNAD (◆), 8,3 nM CNAD (■), or 16.5 nM CNAD (◇). Plots are linear regression fits to the data. However, inhibition constants reported in Table 1 are determined from nonlinear fits to the nonreciprocal forms of the rate equations (see the Experimental Section). (B) Inhibition of alcohol dehydrogenase by CNAD with substrate varied. Ethanol concentrations were varied at a fixed NAD concentration of 100 μM. Assays were performed at pH 8.0 using 2.8 nM ADH in the absence of CNAD (□) or in the presence of 2.5 nM CNAD (◆) or 6.25 nM CNAD (■). Plots are linear regression fits to the data. However, inhibition constants reported in Table 1 are determined from nonlinear fits to the nonreciprocal forms of the rate equations (see the Experimental Section).

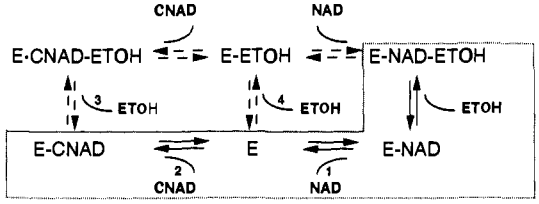

Figure 3. Preferred and minor kinetic mechanisms for ADH (E). Solid arrows indicate the preferred paths (enclosed by the box). Dashed arrows indicate minor paths. Numbers refer to paths discussed in the text.

kinetic constants in Table 1 indicates that CNAD binds to ADH with an ~4–7 kcal/mol lower free energy than it binds to the other dehydrogenases. These data also show that CNAD binds to ADH ~3 kcal/mol more tightly than does the reduced cofactor NADH and ~5 kcal/mol more tightly than the oxidized cofactor NAD. An hypothesis as to the origin of this unusual specificity and affinity can be developed, employing structural information about normal cofactor binding to ADH.

Crystal structures of ADH-bound NAD and NADH have been extensively investigated.[14-18] Of the enzymes listed in Table 1, ADH is unique in having a zinc cation bound at the catalytic site. This zinc atom is coordinated by the sulfurs of Cys 46 and Cys 174 and by the nitrogen of His 67.[14,15] In the absence of bound substrate, the fourth coordination ligand of the zinc is occupied by a water molecule.[14,15] Upon cofactor binding, the nicotinamide end of the cofactor is anchored in the catalytic site by specific hydrogen bonds to the carboxamide group. This positions the cofactor such that the C5 atom of the nicotinamide ring is ~3.6 Å from the catalytic Zn atom (Figure 4a).[15] When substrate binds, it coordinates with the zinc, displacing the water and positioning itself near the nicotinamide ring for hydride transfer.[16]

In CNAD, the pyridine nitrogen occupies the position of the nicotinamide *C5* carbon, the nicotinamide atom closest to the zinc cation. We propose that CNAD mimics normal cofactor binding to ADH. Specifically, we propose that the pyridine ring on ADH-bound CNAD occupies the site normally occupied by the reduced and oxidized nicotinamide ring. In this location, the electron-rich pyridine nitrogen on CNAD is ideally positioned to interact with the zinc cation (Figure 4b).

Similar interactions are observed in crystal structures of inhibitor–ADH complexes containing imidazole and pyrazole.[17,18] In these structures, the heterocyclic nitrogen binds to the catalytic Zn, albeit at the substrate site (below). Whether or not the Zn···N interaction in the CNAD complex is purely electrostatic or forms an actual coordination ligand will depend upon the specific location of the pyridine ring (below). Observation of competitive kinetics with respect to ethanol suggests that CNAD does displace the fourth Zn coordination ligand. In either case, this Zn···N interaction would be expected to stabilize the ADH–CNAD complex. The fact that the zinc cation is present only in ADH would account for both the high affinity and high specificity of CNAD for this enzyme. We offer below kinetic and computational data to support this hypothesis.

ADH–CPAD Binding. Evidence for a specific Zn···N interaction in ADH-bound CNAD is provided by examination of ADH binding by a related inhibitor, CPAD (5-β-D-ribofuranosylpicolinamide adenine dinucleotide, Figure 4c).[6] Like CNAD, CPAD also contains a neutral conjugated pyridine ring in place of the nicotinamide ring found in the normal cofactor. Sterically, CPAD would thus be expected to mimic both NAD and CNAD binding to ADH. Examination of ADH inhibition by CPAD with NAD as the variable substrate shows a competitive pattern of inhibition with a K_i of 21 μM. Thus, CPAD lacks the very high affinity for ADH shown by CNAD, instead binding to the enzyme with an affinity comparable to NAD or NADH (Table 1).

The only difference between CNAD and CPAD is the position of the pyridine nitrogen relative to the carboxamide group. This suggests that the location of this nitrogen in the bound inhibitor is essential in determining whether or not the complex is stabilized beyond that observed for the normal cofactor. The position of the

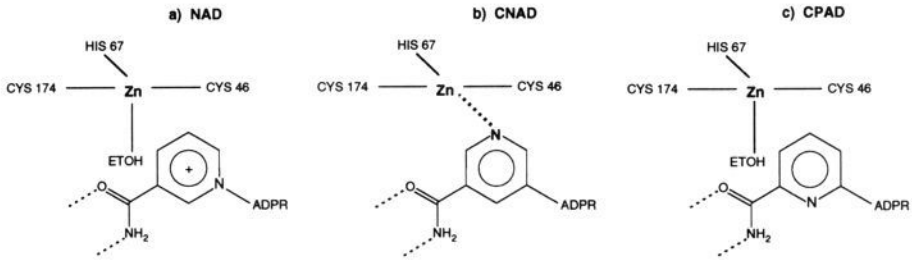

Figure 4. (a) Schematic illustration of the catalytic site in the ternary ADH–NAD^+–ETOH complex. The catalytic zinc is coordinated by Cys 46 and 174, His 67, and water or substrate. Dotted lines to the cofactor carboxamide group represent hydrogen bonds. (b) Schematic illustration of the model of ADH-bound CNAD. The pyridine nitrogen displaces the fourth Zn coordination ligand. (c) Schematic illustration of the model of ADH-bound CPAD, a related analogue.

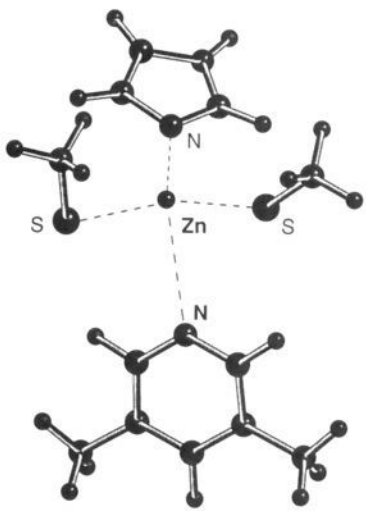

Figure 5. Optimal model used to calculate the enthalpy of formation of the ADH–CNAD complex. This model contains no coordinating solvent, the CNAD nitrogen occupying the fourth ligand on the zinc. Similar models were used to compute the energies of the ADH–NADH and ADH–CPAD complexes, with the exception that these models contained a water molecule coordinated to the Zn at the substrate site. Computed energy differences between the various models are listed in Table 2.

pyridine nitrogen in CPAD is analogous to that of the C2 carbon on NAD. This carbon is 5.6 Å from the zinc cation in ADH-bound NAD. Thus, the pyridine nitrogen on ADH-bound CPAD would be too far from the Zn cation to form any stabilizing interactions (Figure 4c).

Our hypothesis assumes that CNAD mimics cofactor binding to ADH, the only difference being the presence of a N···Zn interaction at the catalytic site in the enzyme-bound inhibitor. The question then arises as to whether or not this N···Zn interaction is of sufficient magnitude to account for the ~3–5 kcal/mol difference in free energy of ADH binding between CNAD and CPAD, NAD, or NADH. The relative magnitude of this interaction can be estimated by a simple computational model, discussed next.

Computational Studies. The computational model assumes that the difference in free energy of binding between CNAD and CPAD or cofactor results primarily from the enthalpic contribution of the N···Zn interaction. This assumption is reasonable for CPAD and NADH but less so for the oxidized cofactor NAD. The solvation energy of the charged nicotinamide ring in NAD is significantly different from that of the uncharged dihydronicotinamide ring in NADH[19] or pyridine rings in CNAD and CPAD. Thus, changes in both enthalpy and entropy upon enzyme binding of NAD will have substantially different contributions from solvent interactions than those seen for the other dinucleotides.

The structures of CNAD, CPAD, and NADH differ only at the dihydronicotinamide and pyridine ends of the molecules, all of which are uncharged. This suggests that relative differences in enthalpy of binding to ADH are due to differences in interactions between the catalytic site on the enzyme and the pyridine or dihydronicotinamide rings on the inhibitors and cofactor, respectively. The relative differences in solvation effects and the entropy of binding for these three species are expected to be similar.

Given the above assumptions, differences in enthalpy of binding between CNAD, CPAD, and NADH were estimated by computing the differences in interaction energy between the pyridine or dihydronicotinamide base on the ligand and the zinc coordination sphere in the catalytic site on ADH. The catalytic zinc was modeled by a divalent zinc cation coordinated to two deprotonated methyl thiols and an imidazole ring (Figure 5). The thiol sulfurs in the model were located at the same positions relative to the zinc as the coordinating sulfurs on Cys 46 and Cys 174 in ADH. The imidazole ring was placed in the same relative position as that of His 67. The fourth zinc coordination site was occupied by a water oxygen, positioned at the ethanol site.

For each ligand base, methyl groups were placed at the positions of the glycosidic and carboxamide bonds (Figure 5). The initial orientation of each base relative to the coordinated zinc was that observed in the crystal structure of the ternary ADH–NAD–dimethyl sulfoxide complex.[16] The energy of formation of each base–Zn "complex" was obtained via *ab initio* quantum mechanical methods by application of the Gaussian 90 program[20] (see the Experimental Section). Molecular mechanics or other pair-potential methods would not sufficiently account for the anisotropy of electronic interactions between the base and the coordinated zinc. The enthalpy of formation of each model was obtained by subtracting the energies of the isolated base and the isolated Zn sphere from that of the entire Zn–base complex. Differences in energy between the CNAD complex and both the CPAD and NADH complexes were then computed and compared with the differences in binding free energies obtained from the kinetic data (see the Experimental Section).

In the initial models, each base was positioned an equivalent distance from the Zn. Differences in calculated enthalpies between these models were not sufficient to account for the observed differences in kinetics. However, the energy of each complex was sensitive to the distance between the coordinated Zn and the nearest atom on the base heterocycle. In the CNAD pyridine, this atom is the nitrogen; hence, any movement of this portion of the

Table 2. Differences in Relative Enthalpies of Formation ($\Delta\Delta E$) between Model Complexes Containing CNAD, NADH, and CPAD (Figure 4)[a]

	$\Delta\Delta E/G_{CNAD-NADH}$ (kcal/mol)	$\Delta\Delta E/G_{CNAD-CPAD}$ (kcal/mol)
calculated $\Delta\Delta E$		
CNAD + H_2O	−0.6	−1.8
CNAD − H_2O	−4.6	−5.8
observed $\Delta\Delta G$	−2.8	−5.1

[a] Models for the NADH and CPAD complexes contained a water molecule coordinated to the Zn at the substrate site. The CNAD complex was modeled both with and without a water molecule coordinated to the Zn at the substrate site (CNAD + H_2O and CNAD − H_2O, respectively). Computed values ($\Delta\Delta E$) are compared with free-energy differences ($\Delta\Delta G$) derived from the kinetic results in Table 1.

heterocycle toward the zinc stabilized the complex. In CPAD and NADH, the atoms closest to the zinc are C–H; hence, any movement of this group toward the zinc destabilized the complex.

Slight changes in the relative orientations of each base were necessary in order to obtain satisfactory agreement between the calculated enthalpy differences and the free-energy differences derived from the kinetics data. The largest adjustment required was a ~0.3-Å shift of the CNAD nitrogen toward the Zn, making the Zn···N distance ~3.2 Å. Computed values are shown in Table 2.

Reasonable agreement between modeled relative enthalpy differences ($\Delta\Delta E$) and observed free-energy differences ($\Delta\Delta G$) is obtained. However, this agreement can only be achieved by removal of the coordinating water ligand in the CNAD model (Table 2, Figure 5). Presence or absence of the water in the CPAD and NADH models (Figure 4) produces only a small (~±0.2 kcal/mol) change in computed values of $\Delta\Delta E$ (data not shown). However, in the presence of the coordinating water oxygen, the CNAD model is significantly destabilized (Table 2). This result is consistent with the kinetic data, suggesting that simultaneous binding of CNAD and ethanol is not favored.

In order to investigate further the origins of the stabilizing interactions in the ADH–CNAD complex, the computational models were subjected to natural bond order (NBO) analysis[21,22] (see the Experimental Section). Results indicate that up to one-half of the energy of stabilization of the model CNAD complex can be attributed to charge transfer interactions, despite the relatively long Zn···N distance observed in the model. As expected, the single largest component of the charge-transfer interaction is due to the overlap of a CNAD nitrogen electron lone pair with unoccupied antibonding orbitals on the zinc. This component increases dramatically as the nitrogen–zinc distance is decreased by even a few tenths of an angstrom, providing further computational support for formation of a Zn···N ligand.

Computational results from these simple models do not account for possible shifts in the positions of the Zn cation or its coordination sphere. This is observed, for example, upon Zn coordination by imidazole.[17] Nor does the model preclude the presence of other protein–ligand interactions. Thus, the CNAD model is not expected to provide an accurate rendering of the detailed geometry of the ADH–CNAD complex. However, computational results are consistent with coordination between the catalytic Zn cation and the pyridine nitrogen at the cofactor site. Results do indicate that this Zn···N interaction in the enzyme–CNAD complex is by itself of sufficient magnitude to account for the very tight binding of CNAD to ADH as well as for the differences in affinity between CNAD and CPAD or NADH.

Comparison with Other ADH Inhibitors. Inhibition of alcohol dehydrogenase provides potential therapies for ethylene glycol intoxication,[23] ethanol-induced hypoglycemia and lactacidemia,[24] and methanol poisoning.[25] This, along with the extensive structural information available on the enzyme and its complexes, has made alcohol dehydrogenase an attractive target for inhibitor design. Pyridine itself is an inhibitor of ADH, albeit a weak one.[26] However, a number of classes of highly potent reversible ADH inhibitors have been developed. These include 4-substituted alkyl pyrazoles,[10,27] 1-mercapto-*n*-alkanes,[28] phenylacetamide and formamide derivatives,[29] and aldoximes.[30] Like CNAD, these inhibitors bind the catalytic site Zn via a nitrogen, oxygen, or sulfur ligand. Unlike CNAD, these compounds act as substrate analogues, binding Zn from the substrate site, with alkyl or phenyl groups extending into the hydrophobic substrate cleft.[18,28-30] Inhibitors of this type can bind in ternary complexes with cofactor, forming a secondary ligand to the nicotinamide ring.[18,30] NAD analogues have been developed as inactivating affinity labels, forming covalent interactions with active-site residues.[31] However, CNAD is likely the first cofactor analogue which reversibly interacts with the catalytic Zn. The most potent alkyl pyrazole, thiol, and aldoxime inhibitors show K_i's of ~0.5 nM.[10,27,28,30] The binding affinity of CNAD to ADH is thus comparable to that of the tightest Zn-binding substrate analogues.[32]

Summary and Conclusions

Kinetic data indicate that the NAD analogue CNAD acts as a general dehydrogenase inhibitor but shows unusual affinity and specificity for alcohol dehydrogenase. Data indicate that, in ADH, CNAD competes for both cofactor and ethanol binding. In ADH, inhibition constants for CNAD are in the nanomolar range with respect to both cofactor and substrate. Thus, CNAD binds to ADH with approximately 3–5 kcal/mol higher affinity than NAD or NADH. Comparison of ADH binding by CNAD and the related analogue CPAD indicates that the position of the pyridine nitrogen has a critical influence on the binding affinity in ADH. The very high affinity and specificity of CNAD for ADH can be explained by a stabilizing interaction between the enzyme's catalytic zinc cation and the pyridine nitrogen on the bound ligand. The binding affinity of CNAD to ADH is comparable to that of other strong ADH inhibitors which coordinate with Zn at the substrate site. Computational models, based on the assumption that the analogues studied here mimic cofactor binding, indicate that an intermolecular Zn···N interaction in ADH-bound CNAD is of sufficient magnitude to account for the observed differences in K_i's. In order to test these models, crystallographic studies of both ADH–CNAD and ADH–CPAD complexes are now underway.

Experimental Section

Materials. CNAD and CPAD were synthesized using the methods described by Pankiewicz *et al.*[6] Horse liver alcohol dehydrogenase was obtained from Sigma Chemical Co., St. Louis, in the lyophilized crystalline form. Pig heart lactate dehydrogenase and the cytoplasmic form of malate dehydrogenase were also from Sigma and were obtained as suspensions in ammonium sulfate. Bovine liver glutamate dehydrogenase was obtained as a solution in 50% glycerol.

All enzymes were diluted to the required stock concentrations using a stock buffer of the same pH and composition as the stock buffer used for each series of assays. Concentrations of the stock enzyme solutions were determined spectrophotometrically using published extinction coefficients at 280 nm.[12,33-35] Enzyme solutions were made on the day of use.

Cofactors (NAD and NADH) were obtained from Sigma Chemical Co. Concentrations of stock solutions were determined spectrophotometrically using published extinction coefficients. Substrates were obtained from Sigma and prepared fresh for use. Concentrations of substrate solutions were calculated from the molecular weight of the compound. All solutions were made up using 18 MΩ water from a Millipore system.

Dehydrogenase Assays. Rate measurements for each of the dehydrogenases used in this study are based on the spectral properties of NADH. In assays with NAD as a substrate, rates were determined by measuring the increase in absorbance at 340 nm resulting from the conversion of NAD to NADH. Rates, using absorbance measurements, were calculated using an extinction coefficient of 6.22 A mM^{-1} cm^{-1} for NADH.[36]

Alcohol dehydrogenase assays were run at pH 8.0, using 0.1 M sodium phosphate buffer. Glutamate dehydrogenase assays were at pH 7.0 in 0.1 M sodium phosphate buffer, containing 10 μM EDTA. Malate dehydrogenase and lactate dehydrogenase assays were performed at pH 9.0 using 0.05 M Tris-HCl buffer. All kinetic assays were run at least in duplicate.

Values of inhibition constants for all enzymes except ADH were estimated from Lineweaver-Burk plots, using linear regression to obtain values for the slope and intercept of each line. Inhibition was judged to be competitive if the values obtained for the intercepts of the appropriate plots differed by less than three standard deviations as determined by linear regression. Values for the inhibition constant K_i were obtained using the relationship:[9]

$$K_i = [I]/[[S(+)/S(-)] - 1]$$

where $S(+)$ and $S(-)$ are the slopes of the plots in the presence and absence of inhibitor respectively and [I] is the concentration of total added inhibitor. K_m for coenzyme was obtained from the slope and intercept obtained in plots in the absence of inhibitor, using the relationship: K_m = slope/V_{max}.

Values of effective inhibition constants and patterns of inhibition for CNAD binding to ADH were obtained by direct least-squares fits to the nonreciprocal forms of the Michaelis-Menten rate equations.[37] Kinetic data were fit to the following relationships, assuming both competitive and noncompetitive inhibition, respectively:

$$v_o = V_m[A]/[K_m(1 + [I]/K_{is}) + [A]]$$

or

$$v_o = V_m[A]/[K_m(1 + [I]/K_{is}) + [A](1 + [I]/K_{ii})]$$

where v_o is the initial reaction rate, V_m is the maximal rate, and K_m and [A] are the Michaelis constant and concentration of the variable substrate, respectively. The pattern of inhibition considered to best account for the observed data was that giving both the smallest residuals between observed and calculated values and the smallest standard errors in the computed kinetics constants. These are the values reported as apparent K_i's ($K_{i(app)}$) in Table 1. Note, however, that the plots shown in Figure 2 are those obtained from the simple linear regression fit to the data.

In order to estimate the magnitude of nonlinear effects introduced by tight binding by CNAD, apparent K_i's with respect to NAD were also obtained by a fit of kinetic data to Sculley and Morrison's nonlinear rate equation:[38]

$$v_0 = \frac{k_{cat}[A]}{2(K_m + [A])}[[([E] - [I] - K_i')^2 + 4K_i'[E]]^{1/2} - (K_i' + [I] - [E])]$$

where K_i' is the apparent K_i obtained via the nonlinear fit, [E] is the total enzyme concentration, and K_{cat} is the maximum rate of product formation. In this case, [A] is the concentration and K_m is the Michaelis constant of NAD. Derivation of this rate equation assumes the presence of a tight binding inhibitor, i.e., that [I] ≃ [E].

In this experiment, both inhibitor and enzyme concentrations were varied. Initial rates v_o were measured at total concentrations of CNAD ([I]) of 0, 2.1, 8.3, and 16.5 nM and total concentrations of ADH ([E]) of 1.75, 3.5, 8.75, and 17.5 nM. Concentrations of ethanol and NAD were fixed respectively at 1.2 mM and 87 μM at pH 8.0. The apparent inhibition constant with respect to NAD, K_i', was then obtained by nonlinear least-squares fit to the rate equation under the array of experimental conditions employed. The true rate constant K_i was obtained from the apparent rate constant K_i' via the relationship:[38]

$$K_i = K_i'/(1 + [A]/K_m)$$

The rate equations used assume a rapid equilibrium between inhibitor and enzyme. Premixing experiments to examine the possibility of changing saturation of the enzyme by CNAD during initial rate determinations were conducted as follows: in the normal assays, enzyme was added to a mixture containing all other reactants, including cofactor, NAD, and inhibitor. In the alternate mixing experiments, enzyme was preincubated with the inhibitor and ethanol, and the reaction initiated by the addition of the appropriate concentration of NAD. In these experiments, the rate of reaction was followed for a 10-min period to determine whether there was any increase in the reaction rate, as might be expected if tightly bound CNAD dissociates after addition of NAD. Otherwise, all ranges of enzyme, cofactor, ethanol, and inhibitor concentrations were the same as those used in the standard assays (Figure 2).

Lastly, the binding of CNAD to ADH was examined directly by fluorescence quenching in the enzyme-inhibitor complex. Maximum quenching of only 26% was produced by saturating CNAD concentrations, and the high affinity of CNAD for ADH required the use of very low concentrations of enzyme. Nevertheless, an estimate of the dissociation constant of the inhibitor was obtained.

Fluorescence was measured with excitation at 280 nm and emission at 340 nm. Increments of CNAD stock solution from 6.5 to 65 nM ([CNAD]) were added to 16.7 nM alcohol dehydrogenase at pH 8.0, and the fluorescence intensity F was measured. The concentration of bound active sites ($[E]_{bound}$) was calculated from the resulting titration curve at each point, based on the fraction of maximum quenching observed at saturation. Thus, $[E]_{bound} = [E]_{total}(F_o - F)/(F_o - F_s)$, where F_o and F_s are the fluorescence intensities in the absence of inhibitor and at saturation, respectively. The free CNAD concentration ($[I]_{free}$) was obtained by subtraction of the bound inhibitor concentration ($[I]_{bound}$) from the total CNAD concentration ($[I]_{total}$) added at each point. It was assumed that there is one CNAD binding site/subunit and that $[I]_{bound} = [E]_{bound}$. Thus, $[I]_{free} = [I]_{total} - [E]_{bound}$. The dissociation constant (K_d) was obtained by a least squares fit to the saturation curve of bound vs free CNAD from the equation:[39]

$$[E]_{bound} = [E]_{bound}^{max}[I]_{free}/([I]_{free} + K_d)$$

where $[E]_{bound}^{max} = [E]_{total}$.

Computational Studies. Models of ADH-bound CNAD and CPAD were based on the crystal structure of the ternary complex of equine liver ADH with NADH and dimethyl sulfoxide.[16] Coordinates were obtained from the Brookhaven Protein Data Bank.[40] The geometry of the coordinated Zn(II) sphere was derived from the crystal structure as described in the text. Geometries of the methylated dihydronicotinamide and pyridine rings were derived from small molecule structures and optimized by a full *ab initio* geometry optimization at the HF/3-21G level using the Gaussian 90 program.[20] The initial orientation of each heterocyclic base relative to the coordinated Zn cation was the same as that of the nicotinamide ring in the crystal structure. Each base was rotated in ~2° increments around an axis through the two methyl-substituted carbons and a single-point computation performed at each orientation using the LANL1MB basis set. This basis set employs an effective core potential for the metal and a STO-3G basis for the other atoms.[41]

The enthalpy of formation of a model containing base 1, ΔE_1, was obtained by subtracting the total electronic energies of the

isolated methylated base E_{B1} and isolated Zn coordination sphere E_{Zn} from that of the entire Zn–base complex E_{B1+Zn}. Thus,

$$\Delta E_1 = E_{B1+Zn} - (E_{B1} + E_{Zn})$$

Differences in the energies of formation between the CNAD model (ΔE_1) and the CPAD and NADH models (ΔE_2) were then obtained via

$$\Delta\Delta E_{12} = \Delta E_1 - \Delta E_2$$

Final orientations of the rings relative to the Zn were those which gave reasonable agreement between calculated energies of formation and differences in free energies.

The difference in free energies of formation between complexes 1 and 2, $\Delta G_1 - \Delta G_2 = \Delta\Delta G_{12}$, was obtained from the kinetic constants K_1 and K_2 via the expression

$$K_1/K_2 = \exp[-\Delta\Delta G_{12}/RT]$$

In order to determine the specific interactions stabilizing each complex, a detailed natural bond orbital (NBO) analysis was performed on each model using the NBO program incorporated in Gaussian 90.[21,22] NBO analysis allows one to isolate interactive energies due to electron density delocalization, or charge transfer, and to relate these interactions to nonbonded interactions on the basis of bond orbital interaction concepts.[21] In this case, NBO analysis allows one to decompose the total interaction energy between the base heterocycle and the Zn complex, E_{B+Zn}, into a charge-transfer energy and a non-charge-transfer energy. The charge-transfer component is explained in terms of the donation of electron density, usually by a bonding or lone-pair orbital, to an antibonding orbital. The non-charge-transfer energy is the component of the interaction energy due to electrostatic and exclusion-repulsion effects.[21] Although this method of energy decomposition is neither unique nor required by theory, it has the advantage of interpreting the computational results in terms of classical chemical concepts.[21]

Acknowledgment. This work was supported by grants CA-45145 (B.M.G.), CA-33907 (K.W.), GM-42010 (K.P.), and GM-47713 (J.E.B.) from the National Cancer Institute and from the National Institute of General Medical Sciences, National Institutes of Health, U.S. Department of Health and Human Services.

Supplementary Material Available: Listings of nonlinear least-squares fits of CNAD kinetic data to Michaelis–Menten and tight-binding rate equations,[37,38] CNAD-induced ADH fluorescence titration curve, and listings of Browse Quantum Chemistry Database System[42] summaries for *ab initio* computations on model complexes (14 pages). Ordering information is given on any current masthead page.

References

(1) See, for example: Fersht, A. *Enzyme Structure and Mechanism*, 2nd ed.; W. H. Freeman & Co.: New York, 1985; Chapter 11.
(2) Abbreviations used are NAD, nicotinamide adenine dinucleotide; NADH, reduced NAD; CNAD, 5-β-D-ribofuranosylnicotinamide adenine dinucleotide; CPAD, 5-β-D-ribofuranosylpicolinamide adenine dinucleotide; ADH, horse liver alcohol dehydrogenase; GDH, bovine liver glutamate dehydrogenase; MDH, pig heart cytoplasmic malate dehydrogenase; and LDH, pig heart lactate dehydrogenase.
(3) White, H. B., III. Evolution of Coenzymes and the Origin of Pyridine Nucleotides. In *The Pyridine Nucleotide Coenzymes*; Everse, J., Anderson, B., You, K.-S., Eds.; Academic Press: New York, 1982; Chapter 1.
(4) Gebeyehu, G.; Marquez, V. E.; Kelley, J. A.; Cooney, D. A.; Jayaram, H. N.; Johns, D. G. Synthesis of Thiazole-4-carboxamide Adenine Dinucleotide. A powerful Inhibitor of IMP Dehydrogenase. *J. Med. Chem.* **1983**, *26*, 922–925.
(5) Marquez, V. E.; Tseng, C. K. H.; Gebeyehu, G.; Cooney, D. A.; Ahluwalia, G. S.; Kelley, J. A.; Dalal, M.; Fuller, R. W.; Wilson, Y. A.; Johns, D. G. Thiazole-4-carboxamide Adenine Dinucleotide (TAD). Analogues Stable to Phosphodiesterase Hydrolysis. *J. Med. Chem.* **1986**, *29*, 1726–1731.
(6) Pankiewicz, K. W.; Zeidler, J.; Ciszewski, L. A.; Bell, J. E.; Goldstein, B. M.; Jayaram, H. N.; Watanabe, K. A. Synthesis of Isosteric C-Nucleotide Analogues of Nicotinamide Adenine Dinucleotide Containing C-Nucleotide of Nicotinamide or Picolinamide. *J. Med. Chem.* **1993**, *36*, 1855–1859.
(7) $K_m \simeq K_{ia} \simeq K_d$ for dissociation of NAD from ADH at the pH employed. For the remaining enzymes, K_m for NAD is ~(5–10)-fold smaller than K_{ia} (see ref 11).
(8) (a) Cha, S.; Tight Binding Inhibitors I. Kinetic Behavior. *Biochem. Pharmacol.* **1975**, *24*, 2177–2185. (b) Cha, S.; Agarwal, R. P.; Parks, R. E., Jr. Tight Binding Inhibitors II. Non-Steady State Nature of Inhibition of Milk Xanthine Oxidase by Allopurinol and Alloxanthine and of Human Erythrocytic Adenosine Deaminase by Coformycin. *Biochem. Pharmacol.* **1975**, *24*, 2187–2197.
(9) Bell, J. E.; Bell, E. T. *Proteins and Enzymes*; Prentice Hall: New Jersey, 1988; Chapters 13–14.
(10) Dahlbom, R.; Tolf, B.-R.; Åkeson, Å.; Lundquist, G.; Theorell, H. On the Inhibitory Power of Some Further Pyrazole Derivatives of Horse Liver Alcohol Dehydrogenase. *Biochem. Biophys. Res. Commun.* **1974**, *57*, 549–553.
(11) Dalziel, K. Kinetics and Mechanism of Nicotinamide-Nucleotide-Linked Dehydrogenases. In *The Enzymes*, 3rd ed.; 1975; Vol. 11, pp 1–60.
(12) Dalziel, K.; Dickinson, F. M. The Kinetics and Mechanism of Liver Alcohol Dehydrogenase with Primary and Secondary Alcohols as Substrates. *Biochem. J.* **1966**, *100*, 34–46.
(13) (a) Silverstein, E.; Boyer, P. D. Equilibrium Reaction Rates and the Mechanisms of Liver and Yeast Alcohol Dehydrogenase. *J. Biol. Chem.* **1964**, *239*, 3908–3914. (b) Ainslie, G. R.; Cleland, W. W. Isotope Exchange Studies on Liver Alcohol Dehydrogenase with Cyclohexanol and Cyclohexanone as Reactants. *J. Biol. Chem.* **1972**, *247*, 946–951.
(14) Cedegren-Zeppezauer, E. S. Coenzyme Binding to Three Conformational States of Horse Liver Alcohol Dehydrogenase. In *Progress in Inorganic Biochemistry Biophysics: Zinc Enzymes*. Gray, H., Bertini, I., Eds.; Birkhäuser Boston, Inc.: Boston, 1986; Vo.. 1, Chapter 29.
(15) Eklund, H.; Samama, J.-P.; Jones, T. A. Crystallographic Investigations of Nicotinamide Adenine Dinucleotide Binding to Horse Liver Alcohol Dehydrogenase. *Biochemistry* **1984**, *23*, 5982–5996.
(16) Eklund, H.; Plapp, B. V.; Samama, J.-P.; Bränden, C.-I. Binding of Substrate in a Ternary Complex of Horse Liver Alcohol Dehydrogenase. *J. Biol. Chem.* **1982**, *257*, 14349–14358.
(17) Cedegren-Zeppezauer, E. S. Crystal-Structure Determination of Reduced Nicotinamide Adenine Dinucleotide Complex with Horse Liver Alcohol Dehydrogenase Maintained in Its Apo Conformation by Zinc-Bound Imidazole. *Biochemistry* **1983**, *22*, 5761–5772.
(18) Eklund, H.; Samama, J.-P.; Wallén, L. Pyrazole Binding in Crystalline Binary and Ternary Complexes with Liver Alcohol Dehydrogenase. *Biochemistry* **1982**, *21*, 4858–4866.
(19) Cummins, P. L.; Ramnarayan, K.; Singh, U. C.; Gready, J. E. Molecular Dynamics/Free Energy Perturbation Study on the Relative Affinities of the Binding of Reduced and Oxidized NADP to Dihydrofolate Reductase. *J. Am. Chem. Soc.* **1991**, *113*, 8247–8256.
(20) Frisch, M. J.; Head-Gordon, M.; Trucks, G. W.; Foresman, J. B.; Schlegel, H. B.; Raghavachari, K.; Robb, M. A.; Binkley, J. S.; Gonzalez, C.; Defrees, D. J.; Fox, D. J.; Whiteside, R. A.; Seeger, R.; Melius, C. F.; Baker, J.; Martin, R. L.; Kahn, L. R.; Stewart, J. J. P.; Topiol, S.; Pople, J. A. GAUSSIAN 90, *Development Version (Revision F)*; Gaussian, Inc.: Pittsburgh, PA, 1990.
(21) Reed, A. E.; Curtiss, L. A.; Weinhold, F. Intermolecular Interactions from a Natural Bond Orbital, Donor-Acceptor Viewpoint. *Chem. Rev.* **1988**, *88*, 899–926.
(22) Glendening, E. D.; Reed, A. E.; Carpenter, J. E.; Weinhold, F., *NBO 3.0 Program Manual*; Theoretical Chemistry Institute and Department of Chemistry: University of Wisconsin, Madison, WI, 1990.
(23) Baud, F. J.; Bismuth, C.; Garnier, R.; Galliot, M.; Astier, A.; Maistre, G.; Soffer, M. 4-Methylpyrazole may be an Alternative to Ethanol Therapy for Ethylene Glycol Intoxication in Man. *Clin. Toxicol.* **1987**, *24*, 463–483.
(24) Salaspuro, M. P.; Pikkarainen, P.; Lindros, K. Ethanol-induced Hypoglycemia in Man: Its Suppression by the Alcohol Dehydrogenase Inhibitor 4-Methylpyrazole. *Europ. J. Clin. Invest.* **1977**, *7*, 487–490.
(25) Jacobsen, D.; Sebastian, C. S.; Barron, S. K.; Carriere, E. W.; McMartin, K. E. Effects of 4-methylpyrazole, Methanol/ethylene Glycol Antidote, In Healthy Humans. *J. Emerg. Med.* **1990**, *8*, 455–61.
(26) Theorell, H.; Yonetani, T.; Sjöberg, B. On the Effects of Some Heterocyclic Compounds on the Enzymatic Activity of Liver Alcohol Dehydrogenase. *Acta Chem. Scand.* **1969**, *23*, 255–260.
(27) Tolf, B.-R.; Piechaczek, J.; Dahlbom, R.; Theorell, H.; Åkeson, Å.; Lundquist G. Synthetic Inhibitors of Alcohol Dehydrogenase. 4-Substituted Alkyl- and Cycloalkylpyrazoles. *Acta Chem. Scand.* **1979**, *B33*, 483–487.
(28) Miwa, K.; Okuda, H.; Ogura, K.; Watabe, T. Long-Chained 1-Mercapto-*n*-Alkanes as Potent Inhibitors Toward Liver Alcohol Dehydrogenase. *Biochem. Biophys. Res. Commun.* **1987**, *142*, 993–998.

(29) Freudenreich, C.; Samama, J.-P.; Biellmann, J.-F. Design of Inhibitors from the Three-Dimensional Structure of Alcohol Dehydrogenase. Chemical Synthesis and Enzymatic Properties. *J. Am. Chem. Soc.* **1984**, *106*, 3344–3353.
(30) Sigman, D. S.; Frolich, M.; Anderson, R. E. Aldoximes: Active-Site Probes of Alcohol Dehydrogenases. *Eur. J. Biochem.* **1982**, *126*, 523–529.
(31) Woenckhaus, C.; Jeck, R. Preparation and Properties of NAD and NADP Analogs. In *Coenzymes and Cofactors, Part A: Pyridine Nucleotide Coenzymes: Chemical, Biochemical and Medical Aspects*; Dolphin, D., Poulson, R., Avramović, O., Eds.; John Wiley and Sons: New York, 1987; Vol. II, pp 541–548.
(32) Metabolic and transport properties of CNAD are under investigation. Effective intracellular concentrations of comparable thiazole dinucleotides can be achieved by the use of either nucleoside precursors or dinucleotide phosphonate analogues. See, for example, citation 5.
(33) Egan, R. R.; Dalziel, K. Active Centre Equivalent Weight of Glutamate Dehydrogenase from Dry Weight Determinations and Spectrophotometric Titrations of Abortive Complexes. *Biochim. Biophys. Acta* **1971**, *250*, 47–49.
(34) Niekamp, C. W.; Hinz, H.-J.; Jaenicke, R.; Woenckhaus, C.; Jeck, R. Correlations between Tertiary Structure and Energetics of Coenzyme Binding in Pig Heart Muscle Lactate Dehydrogenase. *Biochemistry* **1980**, *19*, 3133–3152.
(35) Ladola, A.; Spragg, S. P.; Holbrook, J. Malate Dehydrogenase of the Cytosol. Preparation and Reduced Nicotinamide Adenine Dinucletide-Binding Studies. *Biochem. J.* **1978**, *169*, 577.
(36) Kaplan, N. O. The Pyridine Coenzymes. In *The Enzymes*, 2nd ed.; Boyer, P. D., Lardy, H., Myrback, K., Eds.; Academic Press: New York, 1960; Vol. III, pp 105–169.
(37) Cleland, W. W. Statistical Analysis of Enzyme Kinetic Data. *Methods Enzymol.* **1979**, *63*, 103–138.
(38) Sculley, M. J.; Morrison, J. F. The determination of kinetic Constants Governing the Slow, Tight-binding Inhibition of Enzyme-Catalysed Reactions. *Biochim. Biophys. Acta* **1986**, *874*, 44–53.
(39) Bell, J. E. Fluorescence: Solution Studies. In *Spectroscopy in Biochemistry*; Bell, J. E., Ed.; CRC Press: Boca Raton, FL; Vol. I, pp 155–194.
(40) Bernstein, F. C.; Koetzle, T. F.; Williams, G. J. B.; Meyer, E. F.; Brice, M. D.; Rodgers, J. R.; Kennard, O.; Shimanoucki, T.; Tasumi, M. The Protein Data Bank: A Computer-Based Archival File for Macromolecular Structures. *J. Molec. Biol.* **1977**, *112*, 535–542.
(41) Wadt, W. R.; Hay, P. J. *Ab initio* Effective Core Potentials for Molecular Calculations. Potentials for main group elements Na to Bi. *J. Chem. Phys.* **1985**, *82*, 284–298.
(42) Frisch, M. J. *Browse Quantum Chemistry Database System User's Guide*. Gaussian, Inc.: Pittsburgh, PA, 1988.